water

MDPI

Article

Time Series Analysis for the Adaptive Prediction of Total Phosphorus in the Yangtze River: A Machine Learning Approach

Tianqi Ma [1,2] and Xing Chen [1,2,*]

[1] School of Environment and Energy Engineering, Anhui Jianzhu University, Hefei 230601, China; x22201029@ahu.stu.edu.cn
[2] Anhui Province Engineering Research Center for Mine Ecological Remediation, Anhui University, Hefei 230601, China
* Correspondence: 15705610332@163.com

Abstract: Accurate prediction of total phosphorus (TP) in water quality is critical for monitoring ecosystem stability and eutrophication status. However, the distribution of natural environmental data such as total phosphorus (TP) in water quality tends to undergo complex changes over time. Stable and reliable prediction results not only require a certain degree of stability and periodicity of natural data but also require that the TP prediction model be highly adaptable to random fluctuations and distributional drifts of environmental data. Therefore, it is a challenge to adapt prediction models to the distributional drift of natural environmental data. In this study, the spatial and temporal variations in TP in the Yangtze River from 2019 to 2023 were described in detail. Using data mining techniques, time series data were analyzed to generate a forecast dataset focusing on the stability and periodicity of TP fluctuations. By comparing various time series prediction models, MTS-Mixers was finally selected as the experimental baseline model and different modes were used for time series prediction. The results show that after parameter adjustment, the model can achieve high prediction accuracy (MAE: 0.145; MSE: 0.277), which can guarantee the accuracy at 20 time steps. These research results not only comprehensively described and reliably predicted the changes in TP in the Yangtze River but also provided effective methods and tools for water quality monitoring and management. They provide a scientific basis for environmental protection and water quality improvement in the Yangtze River Basin which can help in the formulation and implementation of relevant policies and promote the sustainable development of the Yangtze River water environment. In addition, this study confirms the applicability of machine learning in hydrological prediction for responding to environmental changes.

Keywords: TP; time series analysis; machine learning; Yangtze River

Academic Editor: Christos S. Akratos

Received: 22 January 2025
Revised: 8 February 2025
Accepted: 16 February 2025
Published: 19 February 2025

Citation: Ma, T.; Chen, X. Time Series Analysis for the Adaptive Prediction of Total Phosphorus in the Yangtze River: A Machine Learning Approach. *Water* **2025**, *17*, 603. https://doi.org/10.3390/w17040603

1. Introduction

Phosphorus (P) is a crucial nutrient essential for crop growth and is also a non-renewable resource. Improper use of phosphorus fertilizers and organic phosphorus pesticides in crop production can lead to excessive phosphorus leaching into adjacent water bodies [1]. Phosphorus in aquatic environments serves as both an important nutrient and a pollutant that can lead to water pollution and ecological issues. Firstly, the limiting factor for the eutrophication of water bodies varies in different environments, but in normal freshwater systems, phosphorus is its main limiting factor [2]. Excessive phosphorus can trigger the growth of harmful algal blooms, leading to phenomena such as red tide and disrupting the ecological balance of water bodies. Secondly, high concentrations of phosphorus exhibit

direct toxicity to aquatic organisms, potentially causing poisoning and mortality in fish and other aquatic life forms [3,4]. Due to rapid population growth and changes in dietary habits in China [5], coupled with intense industrial and agricultural activities, phosphorus has become one of the fastest-growing pollutants in certain basins of China [6,7]. The significant accumulation of phosphorus in the environment also reflects the depletion and overexploitation of phosphorus resources [8]. In seeking a balance between environmental protection and social development, there is increasing attention paid to the changing trends in phosphorus in water bodies and the predictability of phosphorus content.

In the current context of environmental conservation and water resource management, it is crucial to analyze and accurately predict trends in water quality changes [9]. In recent years, with the development of computer and information technology, machine learning has become one of the hottest research directions due to its ability to handle massive amounts of data, as well as due to its high flexibility and adaptability [10]. In the field of natural sciences, machine learning is widely used in various areas of research, including water and air quality monitoring [11,12], environmental pollution source tracking [13], image interpretation [14,15], and geostatistical analysis [16]. Based on different algorithms, machine learning can achieve various objectives. Relevant studies indicate that the Support Vector Machine (SVM) algorithm can be utilized for the isotopic composition of nitrate nitrogen [17], this study significantly reduces the cost of nitrogen isotope detection. Self-Organizing Map Neural Networks (SOM) can be used for identifying the sources of heavy metals in soil [18]. Through the SOM algorithm, different heavy metals are clustered and analyzed for their sources by integrating the different source components provided by the PMF receptor model. Random Forest (RF) [19,20] has also been employed for various classification and regression tasks. Furthermore, the analysis of time series data using machine learning algorithms is currently a focal point of research. Machine learning models can predict future trends or outcomes by learning from historical data, which are of significant importance in natural science research. For instance, Transformers can be utilized to forecast future trends in climate change [21]. Cascade forward net and radial basis function networks, among other neural network algorithms, can also be used for predicting water quality indices [22]. However, currently, there are still shortcomings in research on predicting water quality changes based on time series data in the field of aquatic environment studies [23]. On one hand, issues such as the imbalance in accessibility of water quality data, as well as limitations in temporal and spatial frequency, have resulted in relatively few studies on the application of time series prediction algorithms in water quality forecasting [24,25]. On the other hand, existing research on time series forecasting through machine learning methods tends to focus more on the tuning of algorithms and models and the application of the forecasting results, while neglecting the analysis of the predictability of the time series data themselves.

Water is a necessary condition for human survival, serving as the material basis for agriculture and industrial production, as well as a crucial support for enriching biodiversity and maintaining ecological balance. The Yangtze River is the largest river in China, boasting 40% of the country's usable freshwater resources. It is abundant in water resources and serves as a vital link between terrestrial and marine ecosystems [26]. The Yangtze River Basin is characterized by various sources of phosphorus pollution, including sewage discharge, mineral development, and agricultural and livestock emissions [27]. Complex pollution sources, diverse ecological environments, and climate change make it challenging to predict the variations in phosphorus content in the water of the Yangtze River. Currently, there remains a significant gap in conducting long-term time series analysis and trend prediction for phosphorus in the Yangtze River Basin. To understand the spatiotemporal variations in TP in the Yangtze River, and to forecast its future trends, this study conducted

uninterrupted monitoring over a period of 5 years using evenly spaced intervals. On the one hand, factors such as water temperature, pH, turbidity, dissolved oxygen, and electrical conductivity influence the solubility, forms, and bioavailability of phosphorus, thereby playing a significant role in the concentration of total phosphorus (TP) and the eutrophication process in water bodies. On the other hand, considering that the selected features should be easily collected and detected, it is important to ensure the generalizability of the model. This study systematically examined the water temperature, pH, turbidity, dissolved oxygen, conductivity, and total phosphorus in the main stream of the Yangtze River (104° E to 122° E). Employing various machine learning models, this study analyzed the historical patterns of TP in the Yangtze River and independently predicted TP levels. Additionally, joint predictions were conducted using conventional water quality indicators as features and TP as the target. Deep learning models were established for TP prediction in water quality. This study can provide scientific decision support and technical applications for optimizing water quality prediction and monitoring in river systems.

2. Materials and Methods

2.1. Study Area

The Yangtze River, China's longest river, spans approximately 6300 km in length and covers a basin area of around 1.8 million square kilometers. It flows through 11 provinces, municipalities, and autonomous regions in China, traversing diverse terrains including high mountains, hills, and plains. The region exhibits various climate types, including temperate continental climate, subtropical monsoon climate, and highland mountain climate. The Yangtze River experiences low water levels from October to April of the following year, while the period from May to September sees high water levels [28]. Summer is hot and humid, while winter is damp and cold. The annual precipitation is approximately 1050 mm yr^{-1}, with abundant rainfall [27]. These climatic conditions greatly promote the growth and development of crops, but they also pose certain challenges for water resource management in the region. The abundant water resources along the river make it an important agricultural and industrial base in China [27,29]. The region boasts a developed industrial system and abundant resource advantages, encompassing multiple industries such as automobile manufacturing, electronic information, steel, chemicals, and textiles [30]. The Yangtze River, as China's most important waterway, runs through the region, with numerous ports and docks along its banks, making it a vital inland water transportation hub. However, the ecological environment in the Yangtze River region has been affected by industrialization, urbanization, and intensive land use, resulting in issues such as soil erosion and water pollution [31]. The excessive accumulation of phosphorus in water bodies may contribute to the ongoing issue of eutrophication in certain tributaries, lakes, and estuaries of the Yangtze River basin [32–34]. The Chinese government has implemented a series of policies for the protection and management of the Yangtze River, such as the "Yangtze Three Phosphorus Special Inspection and Rectification Action Implementation Plan" [35] or the "Yangtze River Protection Law" (https://www.gov.cn/xinwen/2020-12/27/content_5573658.htm URL (accessed on 27 January 2025)), committed to improving and protecting the ecological environment of the Yangtze River Basin. As one of China's important river systems, studying the temporal variations in TP in the Yangtze River Basin is of significant importance for addressing issues related to water resource management, ecological conservation, pollution monitoring, and more. From 1961 to 2020, the precipitation in the Yangtze River Basin generally showed an upward trend (an average annual increase of 1.575 mm), but the runoff volume of the Yangtze River decreased by 0.2–2.5% due to the impacts of human activities (e.g., reservoir storage, soil and water conservation, etc.). The decrease from 2001 to 2020 was the most significant [36].

This study holds important value for promoting the economic development of the Yangtze River basin while achieving harmonious development between economy and ecology.

2.2. Sample Collection and Pretreatment

The dataset was derived from a systematic survey conducted by the Yangtze River Mobile Monitoring Vessel (YRMMV), which sampled 2800 km of the Yangtze River mainstem from Yibin (29° N, 104.5° E) to Shanghai (30.5° N, 122° E) (Figure 1). The main site selection included (1) representative hydrological zones (upstream, midstream, and downstream); (2) anthropogenic influence gradients (urban–industrial agglomerations, agricultural zones, and protected areas); and (3) important confluence points with major tributaries. Between January 2019 and December 2023, the vessel maintained a 30- ± 3-day cruise cycle with a 2 h sampling interval. The advantages of the mobile platform are threefold: first, its 5-year operational span captures seasonal and interannual variability; second, the vertical continuity addresses pollutant dispersion patterns that are not accessible to stationary monitoring; and third, the adaptive sampling routes achieve targeted coverage of known pollution hotspots (e.g., Chengdu–Chongqing urban agglomeration, Three Gorges Reservoir area) and ecologically sensitive areas (e.g., Jiangxi Freshwater Dolphin Protection Area). The required parameters were measured using a water quality auto analyzer (MS6100, HACH, Loveland, CO, USA) and included total phosphorus, pH, turbidity, dissolved oxygen, and conductivity. The detection process strictly followed the standards of (HJ/T 103-2003 [37], HJ/T 96-2003 [38], HJ/T 98-2003 [39], HJ/T 99-2003 [40], and HJ/T 97-2003 [41]). Water temperature was measured using a water level temperature gauge (Solinst201, Solinst, Georgetown, ON, Canada), and the measurement procedure followed the guidelines of (GB 13195-91 [42]).

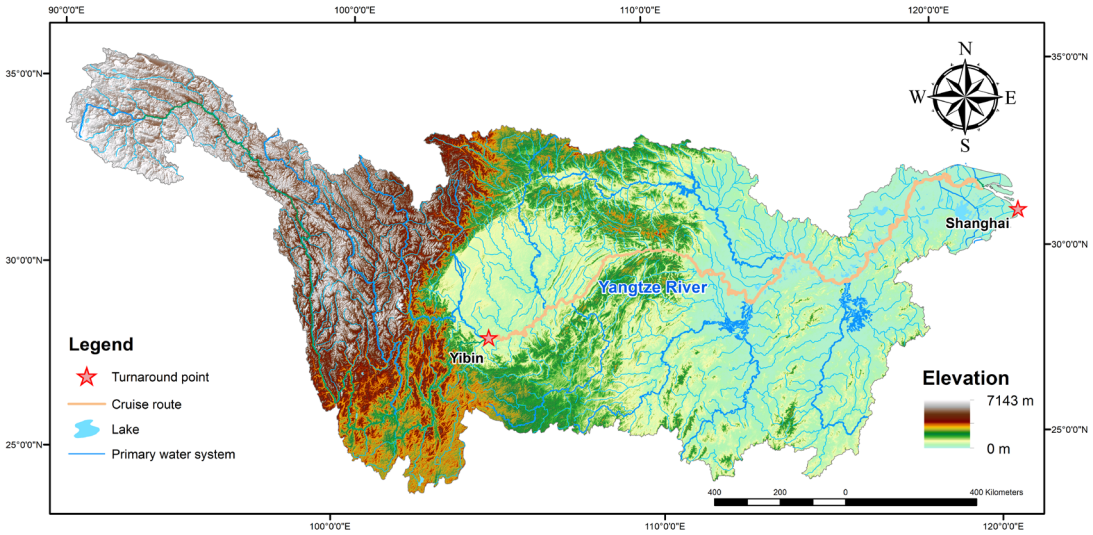

Figure 1. Research area.

The collected data underwent preprocessing, which included data cleaning, integration, transformation, and reduction. The data cleaning process involved removing or filling missing values and outliers. Subsequently, data collected from multiple monitoring cruises were integrated. Normalization and standardization were applied to the data, and feature selection or extraction techniques were employed to reduce the dimensionality of the dataset. The data preprocessing work follows the following principles [19]: 1. Parameters should be reported in the literature to have direct or indirect interactions with total phosphorus, and their data should be readily accessible and detectable in the study. 2. Features that exhibit minimal impact on the simulation effect can be excluded. 3. To

comprehensively consider feature parameters, some features that contribute less to the model's performance should be selectively retained. 4. The basic characteristics of the time series dataset, including trends, seasonality, periodicity, etc., should be thoroughly investigated, and data should be filtered to determine timestamps.

The dataset created in this study comprises one column of timestamps, five columns of feature values, and one column of target values. The time span ranges from 28 January 2019 to 13 December 2023, with a temporal resolution of 'daily'. All timestamps are based on the UTC+8 time zone. The total sample size is 1780 with a dimension of 6, containing one column of target values with five columns of eigenvalues. The five columns of feature values are selected as follows: water temperature (T), pH, turbidity (NTU), dissolved oxygen (DO), and electrical conductivity (EC) [43,44]. The target value is TP. The data in this study are unpublished data from the Chinese Research Academy of Environmental Sciences (CRAES).

2.3. Time Series Analysis Methods

The unit root test is an important concept in time series analysis [45]. It is primarily used to test whether a time series has a unit root, thus determining if the time series data are stationary. Stationarity is one of the fundamental assumptions of many time series analysis methods. Under stationarity conditions, the statistical properties of the time series, such as mean, variance, and autocorrelation structure, do not significantly change over time, this makes the models more robust and reliable. This study utilizes the Augmented Dickey–Fuller (ADF) test method to perform unit root tests on the time series data of TP. The ADF test is used to determine whether a sequence has a unit root: if the sequence is stationary, there is no unit root; otherwise, a unit root exists. Therefore, the null hypothesis (H0) of the ADF test is the presence of a unit root. If the calculated test statistic falls below the critical values at all three conventional significance levels (α = 0.10, 0.05, and 0.01), this provides progressively stronger evidence to reject the null hypothesis. Specifically, the null hypothesis can be rejected at the 10% significance level (90% confidence), 5% significance level (95% confidence), and most stringently at the 1% significance level (99% confidence). The hierarchical relationship between these thresholds indicates that surpassing stricter critical values (e.g., α = 0.01) inherently satisfies the rejection criteria for more lenient thresholds (α = 0.05 and 0.10) in a left-tailed test configuration [46].

The assumption is that future short-term TP measurements can be predicted from historical TP data. The trained model is designed to approximate the functional relationship between past TP measurements and future TP measurements. Therefore, the functional relationship of the TP time series can be described as

$$X_t = \rho X_{t-1} + \mu_t \tag{1}$$

If the random disturbance term μ_t is an m-order autoregressive process (X_t is the value at time cell t)

$$\mu_t = \sum_{i=1}^{m} \beta_m \mu_{t-m} + \epsilon_t \tag{2}$$

In the case where the null hypothesis $\rho = 1$ and $\mu_t = X_t - X_{t-1}$ is satisfied, let $\delta = \rho - 1$, $m \in R$, then

$$X_t - X_{t-1} = \delta X_{t-1} + \sum_{i=1}^{m} \beta_m \left(X_{t-m} - X_{t-m-1} \right) + \epsilon_t \tag{3}$$

The discrete difference equation is

$$\Delta X_t = \delta X_{t-1} + \sum_{i=1}^{m} \beta_1 \Delta X_{t-1} + \epsilon_t \tag{4}$$

Furthermore, this study employed autocorrelation and partial autocorrelation analysis to examine the stability and periodicity of the data.

2.4. Time Series Forecasting Methods

The time series forecasting model developed in this study adopts the MTS-Mixers model developed by Li [47] as the benchmark model. Differing from the attention mechanism in traditional time series forecasting, MTS-Mixers utilizes a decomposition strategy based on time and channel factors to exploit the low-order characteristics of existing time series data, thereby achieving improved forecasting accuracy and efficiency. The overall architecture of the MTS-Mixers model can be simplified by the following three equations:

$$X_h^T = Tomporal(norm(X_h)), X_h^C = Channel\left(X_h + X_h^T\right),\ X_f = Linear\left(X_h^T + X_h^C\right) \quad (5)$$

where X_h represents historical multivariate time series instances and X_f represents the target of the time series forecasting task.

This study selects the MTS-Mixers model as the experimental benchmark and compares it with models based on dynamic linear (DLinear), self-attention mechanism (SCINet), fully connected neural networks (ConvFC), and Fourier transform (FNet) for evaluation and comparison. To ensure the effectiveness of model accuracy evaluation, this study maintains consistency with the overview paper of the MTS-Mixers model in terms of accuracy evaluation methods, employing the MAE, MSE, MAPE, and NRMSE techniques for accuracy assessment. The calculation methods for MAE, MSE, MAPE, and NRMSE are as follows:

$$MAE = \frac{1}{m}\sum_{i=1}^{m}|y_i - \hat{y}_i| \quad (6)$$

$$MSE = \frac{1}{m}\sum_{i=1}^{m}(y_i - \hat{y}_i)^2 \quad (7)$$

$$MAPE = \frac{100\%}{m}\sum_{i=1}^{m}\left|\frac{y_i - \hat{y}_i}{y_i}\right| \quad (8)$$

$$NRMSE = \frac{\sqrt{\text{MSE}}}{\text{Mean}(y_i)} \quad (9)$$

where m is the number of samples, y_i represents the predicted value for i, and $\hat{y}_i$ represents the actual value for i. Lower values of MAE, MSE, MAPE, and NRMSE indicate better model performance.

The in-depth architectures of other models can be found in the Supplementary Information (SI S1). Throughout the experimental process, strict adherence was maintained to the original implementation of the MTS-Mixers model, with appropriate adjustments and extensions made according to the requirements of our study (Figure 2).

2.5. Data Processing Python

The data cleaning, data mining, time series analysis, time series forecasting, and accuracy evaluation involved in this study were all conducted using Python 3.11. The unit root test was conducted using StataMP17, while thematic mapping was created using ArcGIS 10.8. The charts were prepared using Origin 2023. The Supporting Information contains details regarding Python-related compilers, environments, computer models, and other relevant specifications (SI S2).

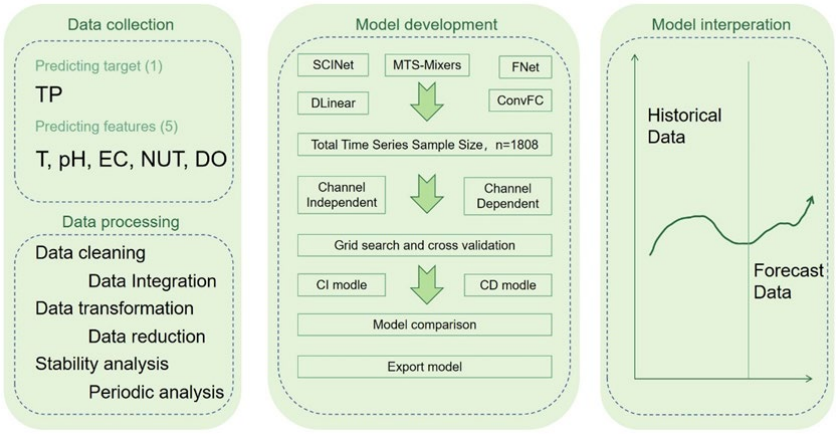

Figure 2. The methodological flow of this experiment.

3. Results and Discussion

3.1. Spatiotemporal Variations of TP in Yangtze River

Table 1 summarizes the physicochemical indicators of surface water quality data in the study area. The pH values of surface water in the study area ranged from 3.42 to 10.13, with the majority of samples exhibiting neutral or weak alkalinity, except for a few samples which showed moderate acidity or moderate alkalinity. The water temperature ranged from 5.6 to 42.1 °C, with 80% of the temperatures falling between 15 and 26 °C, exhibiting a coefficient of variation of 0.265. There were no significant spatial or temporal differences in water temperature in the Yangtze River, indicating favorable conditions for freshwater biological survival [48]. The dissolved oxygen (DO) content of surface water ranged from 1.80 to 11.39 mg/L, with 55% of surface water samples having a DO content greater than 7.5 mg/L (or a saturation rate exceeding 90%). Overall, the surface water of the main stream of the Yangtze River is in an oxidized state. The electrical conductivity (EC) of surface water ranged from 0 to 2907 µS/cm. Lower EC values indicate relatively clean water in the Yangtze River, suggesting the presence of some groundwater recharge [49]. The minimum turbidity value of surface water in the Yangtze River was 0.15 NTU. The maximum value in the dataset significantly deviates from the rest of the data, indicating an outlier. The occurrence of this outlier may be attributed to sediment transport from the riverbed or biological activity during the time of measurement.

Table 1. Summary statistics of routine water quality parameters from the Yangtze River patrol surveys, 2019–2023. Note: 'N' denotes the number of valid data points.

	pH	**T**	**TUB**	**DO**	**EC**
	a.u.	**°C**	**NUT**	**mg L^{-1}**	**µS cm^{-1}**
N	384,861	384,846	384,831	384,870	383,584
Max	10.13	42.10	Outlier	11.39	2907.72
Min	3.42	5.60	0.15	1.8	0.00
Mean	8.159	21.592	46.687	7.67	365.82
Med	8.17	21.92	27.40	7.72	366.60
25%	7.86	16.89	11.50	6.69	329.34
75%	8.47	26.20	50.30	8.7	403.73
CV	0.047	0.265	3.198	0.175	0.219

Table 2 summarizes the integrated data of total phosphorus (TP) in the Yangtze River from 2019 to 2023. In terms of temporal dynamics, the annual average total phosphorus (TP) levels in the Yangtze River follow the sequence 2019 (0.124 mg/L) > 2020 (0.096 mg/L) > 2021 (0.094 mg/L) > 2022 (0.076 mg/L) > 2023 (0.053 mg/L). Overall, the TP content in

the Yangtze River has exhibited a decreasing trend in recent years. Figure 3a depicts the statistical characteristics of total phosphorus (TP) variation in the Yangtze River over the past five years, with the annual variation pattern conforming to the probability density function of a random variable. The violin plot of TP content utilizes kernel smoothing methods, revealing unimodal or multimodal continuous distributions across different years. The central peak is relatively high and gradually decreases towards the tails on both sides, indicating elongated tails and the presence of outliers in the TP content data. The data density is higher near the central peak, gradually decreasing towards the tails on both sides. The violin plot reflects the data characteristics of the dataset in this study, providing reference for subsequent data cleaning tasks. From the perspective of monthly averages (Figure 3b), the TP content in the Yangtze River exhibits higher levels during the wet season and lower levels during the dry season. Precipitation carries away nutrients and pollutants from the surface, including phosphorus from the soil [50,51]. The enrichment of phosphorus in the water bodies of the Yangtze River Basin is closely correlated with precipitation during the warm and rainy season [52].

Table 2. Summary statistics of TP (mg L^{-1}) from the Yangtze River patrol surveys, 2019–2023. Note: 'N' denotes the number of valid data points.

	2019	2020	2021	2022	2023
N	3505	3208	3201	2087	3995
Max	3.364	0.774	0.534	0.858	0.260
Min	0.000	0.000	0.000	0.000	0.009
Mean	0.124	0.096	0.094	0.074	0.053
Med	0.099	0.083	0.089	0.077	0.050
25%	0.079	0.066	0.067	0.045	0.039
75%	0.136	0.109	0.109	0.098	0.070
CV	2.102	0.630	0.487	0.715	0.453

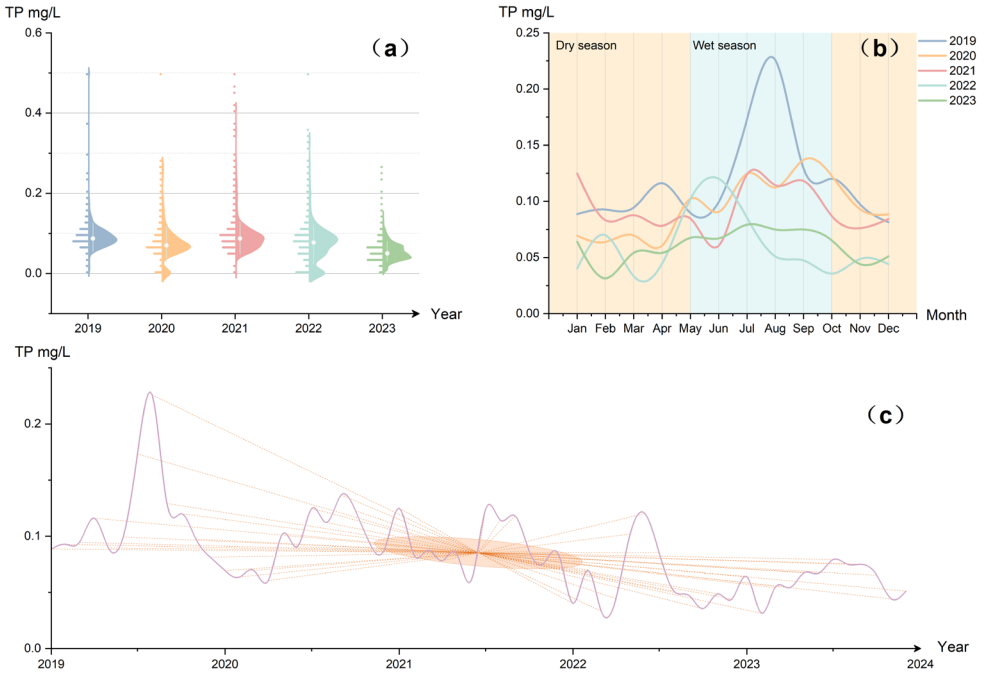

Figure 3. TP time-series variation across years and seasonal scales. (**a**) shows the characteristics of the data distribution for different years; (**b**) demonstrates the seasonal variation in total phosphorus in the Yangtze River; (**c**) demonstrates trends in total phosphorus in the Yangtze River for the period 2019–2023.

3.2. Analysis of the Driving Mechanism of Total Phosphorus Content Changes in the Yangtze River

Monitoring data showed (Figure 3c) a significant trough in total phosphorus concentrations in the Yangtze River during the winter–spring season of 2020–2023, the time dimension of which highly overlapped with the period of COVID-19 outbreak (late 2019) and the period of the implementation of preventive and control measures. The COVID-19 outbreak was accompanied by a series of China-wide closure measures, which resulted in a 58% reduction in population movement in China within 18 days. As a core shipping hub in the middle reaches of the Yangtze River, Wuhan and the Yangtze River Economic Belt implemented preventive and control measures such as industrial closures, transportation restrictions, and bans on public gatherings [53–55], and this particular context verified the direct response relationship between the intensity of human activities and the phosphorus levels in the water body, which provides a rare case of a natural experiment on environmental control.

At the policy implementation level, the 2019 Implementation Plan for the Yangtze River Three Phosphorus Special Examination and Remediation Actions focuses on controlling pollution sources of phosphorus chemical enterprises through the establishment of the "one enterprise, one policy" dynamic supervision system. Especially after the implementation of the "Yangtze River Protection Law" in 2020, a synergistic mechanism of "river chief system + compensation for ecological and environmental damages" will be formed. The decrease in agricultural area, the increase in forestry area, the decrease in fertilizer application, and the decrease in N and P emissions from sewage show the sustained impact of institutional innovation on pollutant control [56,57].

Further analysis revealed that the seasonal fluctuations of total phosphorus changes showed a significant double-driven feature: the increase in phosphorus loading from agricultural surface sources during the spring plowing period (March–May) to the TP entering the water body through surface runoff during the precipitation period (May–August), which resulted in the temporal and spatial coupling of the TP content of the surface water with the seasons. The peak TP amount exhibited in the rainy season (June–August) (0.7–1.6-fold increase compared with the dry season) reveals the dominant seasonal role of nonpoint source pollution.

Ecological restoration projects under the framework of the Yangtze River protection strategy showed progressive regulatory effects: (1) wetland restoration projects enhanced sediment phosphorus fixation capacity [58]; (2) the construction of riparian vegetation buffer zones intercepted surface runoff TP [59]. These engineering measures formed a positive superposition effect with the policy control, driving the TP concentration of the mainstem of the Yangtze River to show a sustained downward trend in the last five years (average annual decreasing rate of 18.5%).

3.3. Time Series Analysis

In order to determine whether the time series data of TP in the dataset have a stable long-term trend or random walk characteristics, the time series of the target value of TP was de-trended with stability and periodicity analysis in this study. Figure 4 illustrates the time series characteristics of the dataset in this study. Among them, Figure 4a illustrates the distribution of the target variable TP in the dataset, where the horizontal axis represents the range of variable values, and the vertical axis represents frequency. The TP data exhibit an overall unimodal asymmetric shape. Data that were not captured or that were captured and determined to be in error and deleted were populated using arithmetic mean interpolation. Figure 4b,c depict the correlation of the target variable TP with itself at different lag periods in the dataset. The horizontal axis represents the lag period, and the vertical axis represents the correlation coefficient. The partial autocorrelation plot (Figure 4c)

provides a more detailed description of the relationship between variables. It eliminates the influence of other lag periods, making it easier to determine the parameters of the time series model [60]. The results indicate that there is a weak positive correlation in TP content data at lag periods of approximately within 15, around 30, and 40. This suggests the presence of some periodicity in the time series, with a period of approximately one cruise cycle (30 ± 5 days). The density is relatively concentrated, and both the autocorrelation and partial autocorrelation function plots show some autocorrelation. The correlation coefficients remain stable at different lag periods, indicating that the TP time series exhibits strong stability.

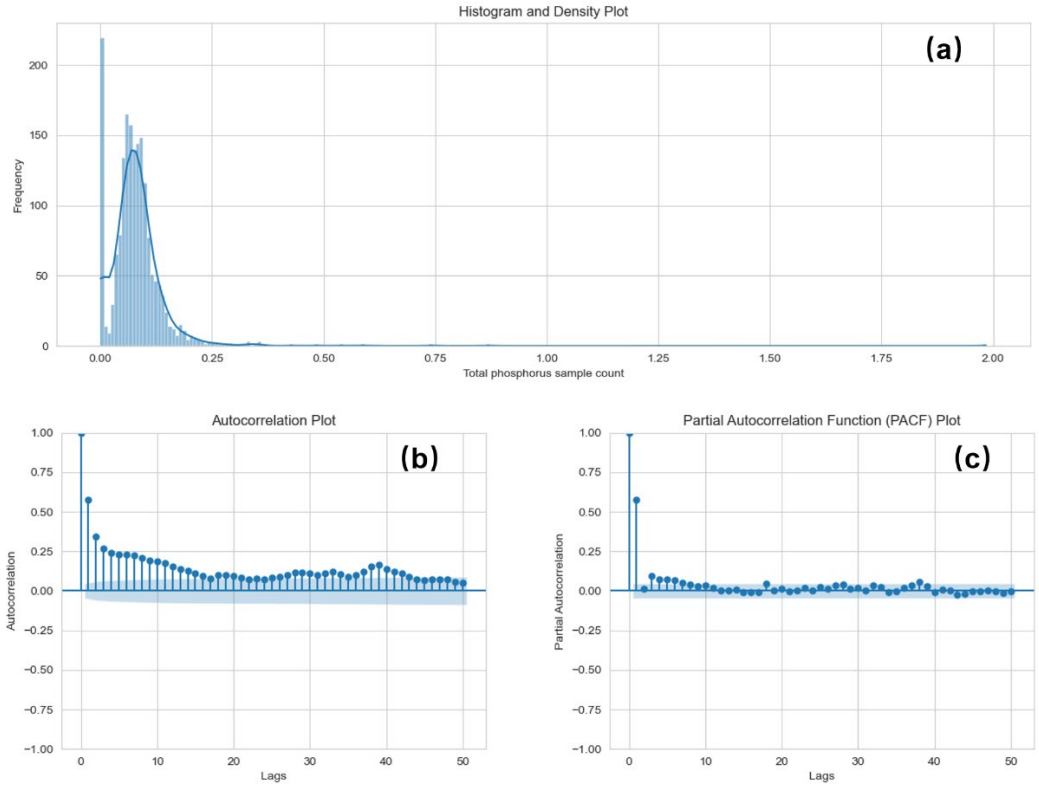

Figure 4. The results of time series analysis show the distribution frequency and autocorrelation of the time series (**a**); the distribution of the target variable TP in the dataset (**b**); and (**c**) the correlation of the target variable TP with itself at different lag periods.

In this study, we also employed the Augmented Dickey–Fuller (ADF) test to examine the stationarity of TP content time series data. Detailed results of the ADF test are provided in the Supplementary Information (SI S3). We calculated the ADF test statistic and compared it with the critical value at the chosen significance level (1%). The computed ADF test statistic is -21.968. At the 1% significance level, the critical value is -3.43. Since the value of the ADF test statistic is less than the critical value, we can reject the null hypothesis. This indicates that the TP time series data in our study do not have a unit root and are stationary. This result is of significant importance for our research, demonstrating the effectiveness of our data cleaning and data mining efforts. Stationary time series data provide a foundation for further time series analysis and modeling [61]. This implies that we can conduct trend analysis, periodicity analysis, or construct prediction models more reliably, allowing for a deeper investigation into the dynamic characteristics of time series data and the underlying relationships with other features.

The decomposition of the TP data (Figure 5) provides a clearer picture of the trend and seasonal fluctuations in TP. In terms of the long-term trend, the TP content shows a stable trend during the rest of the time, except for the existence of extreme values at the

beginning of 2020. In addition, the seasonal change in TP has a certain periodicity. The length of the cycle is about 3 months. The weak periodicity proves that the season is not the main factor affecting the change in its content, and the change in TP content is mainly affected by human activities. The fluctuation of the residual term of TP is stochastic, but the amplitude of the fluctuation is correlated with the original time series to a high degree.

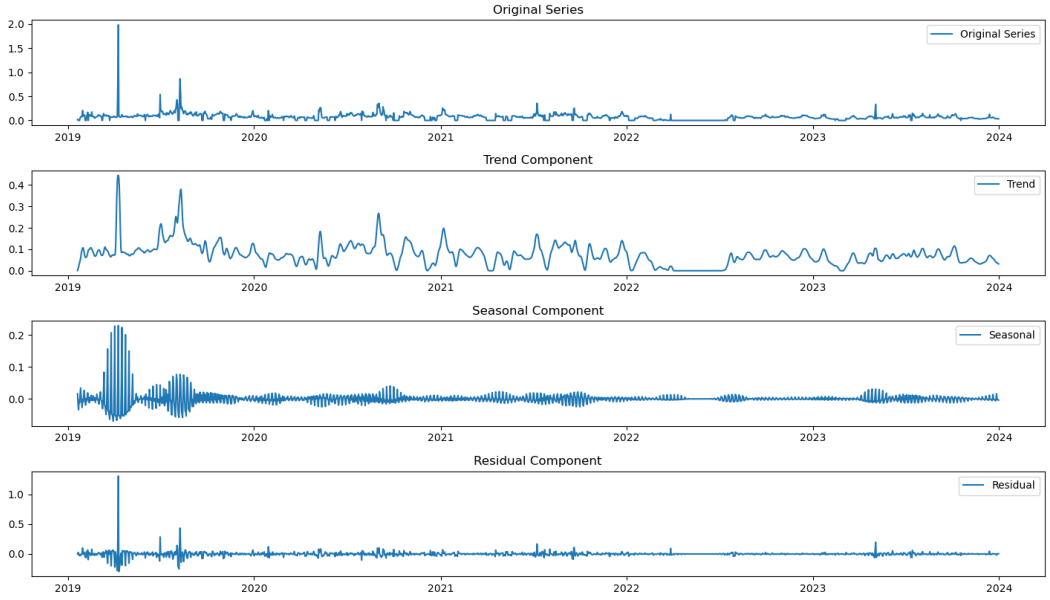

Figure 5. Decomposition results for TP data time series.

3.4. Predictive Model Parameter Tuning and Performance Evaluation

The prediction accuracy of a trained model can only be guaranteed when the distributions of the training data and the data to be predicted are consistent. In consideration of the data collection period and the results of time series analysis, this study employed a grid search with a cruising cycle (approximately 30 days) as a time window to seek the optimal hyperparameters for the input sequence length (seq_len) and the start token length (label_len). The prediction sequence length (pred_len) was set to one cruising cycle. Here, 'input sequence length' indicates the number of data points used to predict future data. Distinguishing itself from other models, the MTS-Mixers model features a parameter named 'start token length'. This parameter denotes the number of data points with higher weights within the data used for prediction. The presence of this parameter enables the model to more effectively identify and leverage crucial information within the data. Optimal learning rate was determined through a gradient-based approach, with Mean Squared Error (MSE) serving as the loss function. Early stopping was implemented to prevent overfitting and preserve the model's generalization ability, halting training when the validation loss ceased to decrease.

Figure 6 compares the prediction accuracies of various time series forecasting models under different time step main hyperparameters (MHs), and the detailed data are shown in Table S1. In this study, cross-validation is performed using a sliding window split time series method, where the window splitter generates folds on a sliding window over time. The results indicate that for independent predictions, the MTS-Mixers model achieved an average MSE of approximately 0.153, which is lower by approximately 0.039 compared to other models, an average MAE of approximately 0.228, lower by approximately 0.44 compared to other models, an average NRMSE of approximately 0.049, lower by approximately 0.008 compared to other models, and an average MAPE of approximately 3.62%, lower by approximately 0.58% compared to other models. The optimal hyperparameters were

determined to be MH2 and MH7. For joint predictions, the MTS-Mixers model attained an average MSE of approximately 0.194, lower by approximately 0.027 compared to other models, and an average MAE of approximately 0.323, lower by approximately 0.045 compared to other models. The optimal hyperparameters were found to be MH4. However, it is noted that the joint prediction accuracy of MTS-Mixers is inferior to that of independent prediction. Overall, the MTS-Mixers model exhibits high prediction accuracy in both univariate and multivariate forecasting, demonstrating lower average prediction errors and biases relative to other models. These findings underscore its superior predictive performance.

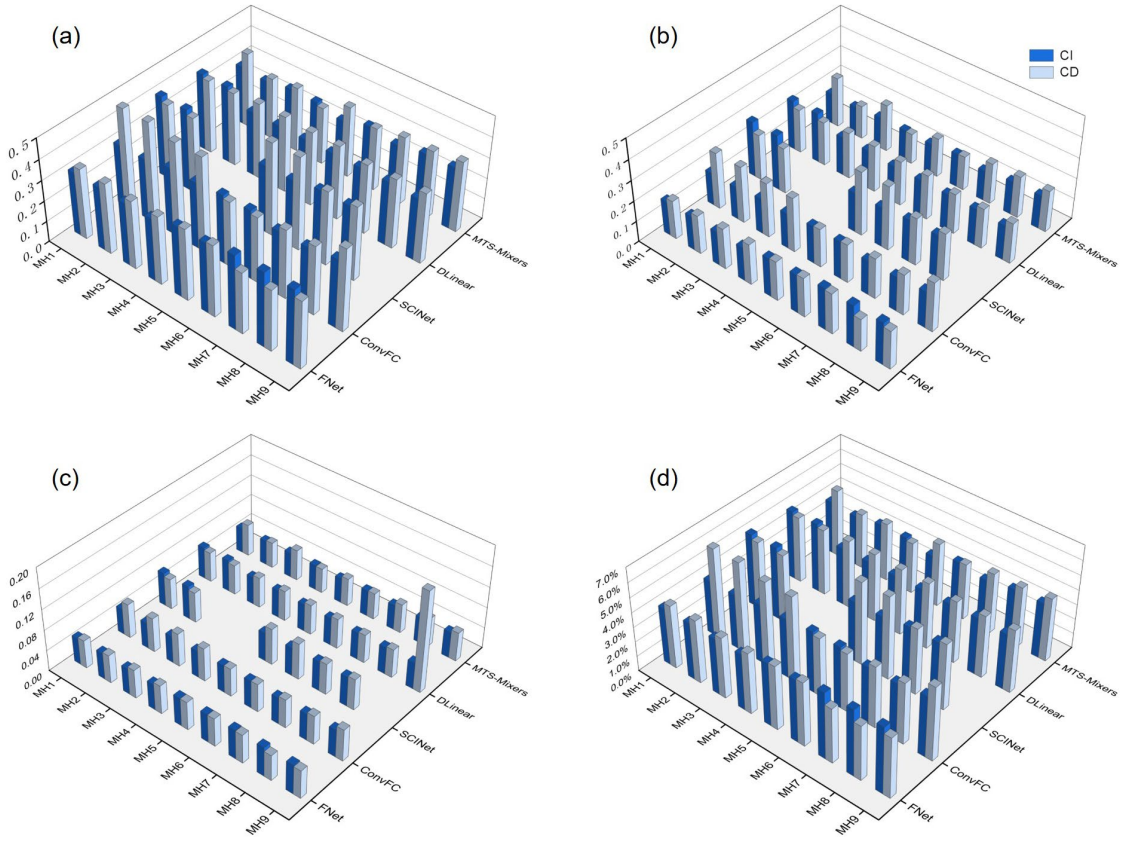

Figure 6. Progress evaluation of different models. (**a**) denotes the MAE of different models, (**b**) denotes the MSE of different models, (**c**) denotes the NRMSE of different models, and (**d**) denotes the MAPE of different models. The smaller the value of both, the higher the model accuracy.

Based on comparisons with other time series prediction tasks, the independent prediction model developed in this study based on MTS-Mixers not only demonstrates higher prediction accuracy and lower prediction errors compared to Long short-term memory (LSTM), Transformer, and Spatio-temporal causal convolutional network (ST-CausalConvNet) [62,63] but also offers a longer time prediction horizon.

In natural environments, data distributions may change over time or due to shifts in the environment, leading to what is commonly known as Distribution Drift in real-world data (also known as Distribution Shifts) [64]. The joint prediction models necessitate the consideration of a greater number of variables and factors, leading to more complex data processing and analysis. Consequently, these factors render joint prediction models more sensitive to Distribution Drift. In contrast, independent prediction only requires consideration of a single target variable, which is generally simpler and more straightforward. Due to the increased data challenges and model complexity associated with joint prediction, it may lead to higher errors and uncertainties, consequently resulting in relatively poorer overall prediction accuracy [65].

Figure 7 displays the actual values of TP data alongside the predicted values of channel independent (CI) and channel dependent (CD), with the time span of the actual values selected based on the optimal start token length (90 days) for both CI and CD, and a prediction time span of 30 days. The predicted curves exhibit a trend, with confidence intervals (CIs) surrounding each prediction curve. These confidence intervals reflect the range of prediction uncertainty. At a 95% confidence level, the confidence interval for CI is approximately 0.0133, while for CD it is approximately 0.0095. The actual value curve serves as a reference to facilitate the comparison of prediction accuracy. By observing the curves and confidence intervals, one can gain a better understanding of the performance and reliability of the prediction model, as well as the differences and trends between actual and predicted values. The results underscore that CI demonstrates better prediction accuracy for this research dataset, and it maintains good predictive performance particularly when the prediction time step is within 20 days. After 20 days, there is a noticeable decrease in prediction accuracy. This phenomenon of declining prediction accuracy as the prediction time progresses is commonly observed in time series forecasting experiments [66,67]. On one hand, the non-stationarity of data, noise, and the introduction of underlying factors can make it challenging for the model to effectively learn long-term memory information. On the other hand, uncertainties in surface water hydrology and the understanding of interactions among various physicochemical indicators may still exceed existing systemic knowledge [68,69].

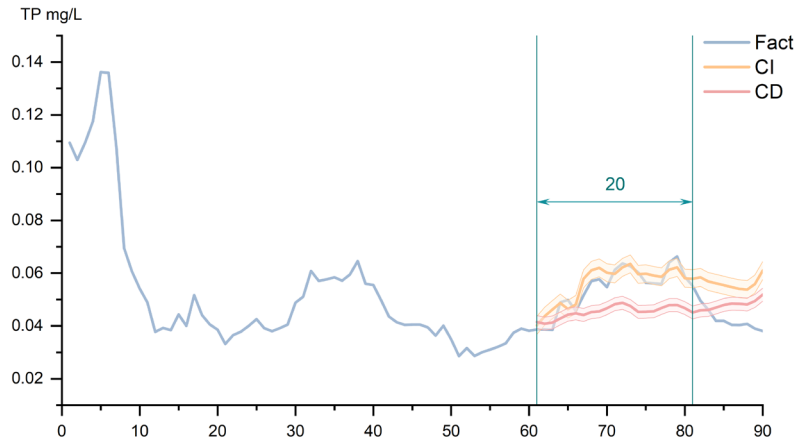

Figure 7. Output results under different model predictions: channel-independent (CI) and channel-dependent (CD).

4. Conclusions and Suggestion

This study describes the spatiotemporal variations in total phosphorus (TP) in the Yangtze River from 2019 to 2023. It involves data cleaning and mining of TP time series data to construct a predictive time series dataset and delves into the stability and periodicity of TP variations within the dataset. By comparing various time series forecasting models, the optimal model MTS-Mixers is selected, and TP is forecasted using both CI and CD modes. Within 20 time steps, the MTS-Mixers model maintains good prediction accuracy for the dataset.

This study not only performs the dynamic analysis and prediction of the spatial and temporal changes in total phosphorus in the Yangtze River basin, but more importantly, the high-precision prediction results outputted by the machine learning model provide a direct basis for the precise policy of water quality management in the basin. Based on the seasonal fluctuation pattern of total phosphorus concentration revealed by the model. For the water quality management and ecological protection of the Yangtze River basin, this study proposes the following measures: (1) During the superposition of the agricultural fertilization period and the rainy season from May to September, an ecological

interception project of agricultural irrigation and water withdrawal should be implemented for the middle and upper reaches of the basin so as to control the amount of surface source pollution into the river. (2) Focus should be placed on the supervision of downstream sewage discharge from populated areas and industrial parks during the dry season to achieve early warning on abnormal discharge through real-time comparison between the online monitoring data and the predicted values. (3) For Poyang Lake, Dongting Lake, and other sensitive water bodies, it is recommended that a red line be set for total phosphorus control (e.g., $\leq$0.10 mg/L). (4) Centralized treatment of aquaculture tail water should be recommended. It is worth noting that, although the current model has a good prediction ability for the progressive pollution process, it is still necessary to establish multiple response mechanisms such as relying on the model to guide the long-term management in the routine period and initiating a rapid response program combining drone inspection and manual sampling in the emergency state for the sudden change in concentration caused by unexpected environmental events (e.g., chemical leakage, impact of heavy rainfall runoff, etc.) [70].

In addition to the models mentioned in the text, this study tried a variety of algorithms, including Informer, FEDformer, Autoformer, etc., during the model selection process in the preliminary experiments. These models are neither good at handling multivariate time-series prediction nor do they fit the dataset of this study well after a series of parameter adjustments (Table S1). The dataset used in this study is not overly time-dependent, i.e., it does not have excessively long time series; earlier data have a greater negative impact on forecasting, and algorithms (e.g., Informer) applied to the task of forecasting time series with long series may not be suitable for this study's dataset. Secondly, this study dataset lacks stochastic fluctuation series with obvious frequency-domain characteristics, and when the object to be analyzed belongs to a completely disordered or pseudo-random process, it may be difficult to obtain valuable information from it by relying solely on spectral transformation techniques (e.g., FEDformer). Furthermore, due to the susceptibility of natural data to issues like data noise and collinearity, joint prediction performs poorly in this study dataset. Joint prediction typically poses greater challenges and difficulties. However, through alternative data processing and feature engineering, optimization of model parameters and algorithm selection, as well as effective model evaluation and improvement strategies, there is still an opportunity to enhance the accuracy of joint prediction and even surpass the performance of independent prediction.

To address these issues, our upcoming research directions include considering the time-domain frequency reconstruction method in electronic information. Through frequency decomposition and reconstruction of time series data, this process can help us better understand the frequency characteristics of time series and play a role in data processing and analysis. With time-domain frequency reconstruction, we can conduct more in-depth and accurate analysis of the data to reveal hidden information and features.

Supplementary Materials: The following supporting information can be downloaded at https://www.mdpi.com/article/10.3390/w17040603/s1, SI S1: Other Models for Comparison; SI S2: Computing Environment; SI S3: Raw Results of ADF Test. Table S1: Evaluation of Accuracy in Independent Prediction and Joint Prediction by Different Models Note: Bold font indicates the best result. Table S2: Models involved in model screening and accuracy evaluation (take the best result). References [71–73] are cited in the Supplementary Materials.

Author Contributions: Writing—original draft, T.M.; Writing—review & editing, X.C. All authors have read and agreed to the published version of the manuscript.

Funding: This work was supported by the Natural Science Foundation of Anhui Province (2208085MD100), Natural Science Research Project of Anhui Educational Committee (2024AH040046, 2022AH050260), and the National Key Research and Development Program of China (2021YFC3201005).

Data Availability Statement: The original contributions presented in this study are included in the article/Supplementary Material. Further inquiries can be directed to the corresponding author.

Conflicts of Interest: The authors declare that they have no known competing financial interests or personal relationships that could have appeared to influence the work reported in this paper.

References

1. Zou, T.; Zhang, X.; Davidson, E.A. Global Trends of Cropland Phosphorus Use and Sustainability Challenges. *Nature* **2022**, *611*, 81–87. [CrossRef] [PubMed]
2. Yang, Y.-Y.; Toor, G.S. Sources and Mechanisms of Nitrate and Orthophosphate Transport in Urban Stormwater Runoff from Residential Catchments. *Water Res.* **2017**, *112*, 176–184. [CrossRef] [PubMed]
3. Yuan, Z.; Jiang, S.; Sheng, H.; Liu, X.; Hua, H.; Liu, X.; Zhang, Y. Human Perturbation of the Global Phosphorus Cycle: Changes and Consequences. *Environ. Sci. Technol.* **2018**, *52*, 2438–2450. [CrossRef]
4. King, W.M.; Curless, S.E.; Hood, J.M. River Phosphorus Cycling during High Flow May Constrain Lake Erie Cyanobacteria Blooms. *Water Res.* **2022**, *222*, 118845. [CrossRef] [PubMed]
5. Tilman, D.; Clark, M. Global Diets Link Environmental Sustainability and Human Health. *Nature* **2014**, *515*, 518–522. [CrossRef] [PubMed]
6. Hu, Y.; Chen, M.; Pu, J.; Chen, S.; Li, Y.; Zhang, H. Enhancing Phosphorus Source Apportionment in Watersheds through Species-Specific Analysis. *Water Res.* **2024**, *253*, 121262. [CrossRef]
7. Lin, S.-S.; Shen, S.-L.; Zhou, A.; Lyu, H.-M. Assessment and Management of Lake Eutrophication: A Case Study in Lake Erhai, China. *Sci. Total Environ.* **2021**, *751*, 141618. [CrossRef]
8. Zhang, C.; Guisasola, A.; Baeza, J.A. A Review on the Integration of Mainstream P-Recovery Strategies with Enhanced Biological Phosphorus Removal. *Water Res.* **2022**, *212*, 118102. [CrossRef]
9. Chang, H. Spatial Analysis of Water Quality Trends in the Han River Basin, South Korea. *Water Res.* **2008**, *42*, 3285–3304. [CrossRef]
10. Yun, D.; Kang, D.; Cho, K.H.; Baek, S.-S.; Jeon, J. Characterization of Micropollutants in Urban Stormwater Using High-Resolution Monitoring and Machine Learning. *Water Res.* **2023**, *235*, 119865. [CrossRef]
11. Qin, X.; Gao, F.; Chen, G. Wastewater Quality Monitoring System Using Sensor Fusion and Machine Learning Techniques. *Water Res.* **2012**, *46*, 1133–1144. [CrossRef] [PubMed]
12. Hu, X.; Belle, J.H.; Meng, X.; Wildani, A.; Waller, L.A.; Strickland, M.J.; Liu, Y. Estimating $PM_{2.5}$ Concentrations in the Conterminous United States Using the Random Forest Approach. *Environ. Sci. Technol.* **2017**, *51*, 6936–6944. [CrossRef] [PubMed]
13. Dávila-Santiago, E.; Shi, C.; Mahadwar, G.; Medeghini, B.; Insinga, L.; Hutchinson, R.; Good, S.; Jones, G.D. Machine Learning Applications for Chemical Fingerprinting and Environmental Source Tracking Using Non-Target Chemical Data. *Environ. Sci. Technol.* **2022**, *56*, 4080–4090. [CrossRef]
14. Liu, Y.; Zhang, Y.; Yu, P.; Ye, T.; Zhang, Y.; Xu, R.; Li, S.; Guo, Y. Applying Traffic Camera and Deep Learning-Based Image Analysis to Predict PM2.5 Concentrations. *Sci. Total Environ.* **2024**, *912*, 169233. [CrossRef]
15. Lian, Z.; Rui, L.; Xuemei, W. The Development and Application of Machine Learning in Atmospheric Environment Studies. *Remote. Sens.* **2021**, *13*, 4839.
16. Yang, J.; Huang, X. The 30 m Annual Land Cover Dataset and Its Dynamics in China from 1990 to 2019. *Earth Syst. Sci. Data* **2021**, *13*, 3907–3925. [CrossRef]
17. Yang, Y.; Shang, X.; Chen, Z.; Mei, K.; Wang, Z.; Dahlgren, R.A.; Zhang, M.; Ji, X. A Support Vector Regression Model to Predict Nitrate-Nitrogen Isotopic Composition Using Hydro-Chemical Variables. *J. Environ. Manag.* **2021**, *290*, 112674. [CrossRef]
18. Zheng, J.; Wang, P.; Shi, H.; Zhuang, C.; Deng, Y.; Yang, X.; Huang, F.; Xiao, R. Quantitative Source Apportionment and Driver Identification of Soil Heavy Metals Using Advanced Machine Learning Techniques. *Sci. Total Environ.* **2023**, *873*, 162371. [CrossRef]
19. Yang, C.; Dong, H.; Chen, Y.; Xu, L.; Chen, G.; Fan, X.; Wang, Y.; Tham, Y.J.; Lin, Z.; Li, M.; et al. New Insights on the Formation of Nucleation Mode Particles in a Coastal City Based on a Machine Learning Approach. *Environ. Sci. Technol.* **2023**, *58*, 1187–1198. [CrossRef]
20. Li, P.; Hua, P.; Zhang, J.; Krebs, P. Ecological Risk and Machine Learning Based Source Analyses of Trace Metals in Typical Surface Water. *Sci. Total Environ.* **2022**, *838*, 155944. [CrossRef]
21. Sietsma, A.J.; Theokritoff, E.; Biesbroek, R.; Canosa, I.V.; Thomas, A.; Callaghan, M.; Minx, J.C.; Ford, J.D. Machine Learning Evidence Map Reveals Global Differences in Adaptation Action. *One Earth* **2024**, *7*, 280–292. [CrossRef]

22. Georgescu, P.-L.; Moldovanu, S.; Iticescu, C.; Calmuc, M.; Calmuc, V.; Topa, C.; Moraru, L. Assessing and Forecasting Water Quality in the Danube River by Using Neural Network Approaches. *Sci. Total Environ.* **2023**, *879*, 162998. [CrossRef] [PubMed]
23. Zhi, W.; Appling, A.P.; Golden, H.E.; Podgorski, J.; Li, L. Deep Learning for Water Quality. *Nat. Water* **2024**, *2*, 228–241. [CrossRef] [PubMed]
24. Zhao, B.; Zhu, W.; Hao, S.; Hua, M.; Liao, Q.; Jing, Y.; Liu, L.; Gu, X. Prediction Heavy Metals Accumulation Risk in Rice Using Machine Learning and Mapping Pollution Risk. *J. Hazard. Mater.* **2023**, *448*, 130879. [CrossRef]
25. McCabe, M.F.; Rodell, M.; Alsdorf, D.E.; Miralles, D.G.; Uijlenhoet, R.; Wagner, W.; Lucieer, A.; Houborg, R.; Verhoest, N.E.C.; Franz, T.E.; et al. The Future of Earth Observation in Hydrology. *Hydrol. Earth Syst. Sci.* **2017**, *21*, 3879–3914. [CrossRef]
26. Chen, X.; Fu, X.; Li, G.; Zhang, J.; Li, H.; Xie, F. Source-Specific Probabilistic Health Risk Assessment of Heavy Metals in Surface Water of the Yangtze River Basin. *Sci. Total Environ.* **2024**, *926*, 171923. [CrossRef]
27. Wang, Z.; Tian, L.; Zhao, C.; Du, C.; Zhang, J.; Sun, F.; Tekleab, T.Z.; Wei, R.; Fu, P.; Gooddy, D.C.; et al. Source Partitioning Using Phosphate Oxygen Isotopes and Multiple Models in a Large Catchment. *Water Res.* **2023**, *244*, 120382. [CrossRef]
28. Meng, L.; Xue, J.; Zhao, C.; Huang, T.; Yang, H.; Zhao, K.; Yu, Z.; Yuan, L.; Zhou, Q.; Kellerman, A.M.; et al. N-Containing Dissolved Organic Matter Promotes Dissolved Inorganic Carbon Supersaturation in the Yangtze River, China. *Water Res.* **2023**, *247*, 120808. [CrossRef]
29. Liu, Q.; Xu, X.; Lin, L.; Bai, L.; Yang, M.; Wang, W.; Wu, X.; Wang, D. A Retrospective Analysis of Heavy Metals and Multi Elements in the Yangtze River Basin: Distribution Characteristics, Migration Tendencies and Ecological Risk Assessment. *Water Res.* **2024**, *254*, 121385. [CrossRef]
30. Zeng, S.; Du, C.; Li, Y.; Lyu, H.; Dong, X.; Lei, S.; Li, J.; Wang, H. Monitoring the Particulate Phosphorus Concentration of Inland Waters on the Yangtze Plain and Understanding Its Relationship with Driving Factors Based on OLCI Data. *Sci. Total Environ.* **2022**, *809*, 151992. [CrossRef]
31. Zhang, Y.; Shen, R.; Gu, X.; Li, K.; Chen, H.; He, H.; Mao, Z.; Johnson, R.K. Simultaneous Increases of Filter-Feeding Fish and Bivalves Are Key for Controlling Cyanobacterial Blooms in a Shallow Eutrophic Lake. *Water Res.* **2023**, *245*, 120579. [CrossRef] [PubMed]
32. Tong, Y.; Bu, X.; Chen, J.; Zhou, F.; Chen, L.; Liu, M.; Tan, X.; Yu, T.; Zhang, W.; Mi, Z.; et al. Estimation of Nutrient Discharge from the Yangtze River to the East China Sea and the Identification of Nutrient Sources. *J. Hazard. Mater.* **2017**, *321*, 728–736. [CrossRef] [PubMed]
33. Liu, W.; Qin, T.; Wu, M.; Chen, Z.; Zhang, Y.; Abakumov, E.; Chebykina, E.; Wang, W.; Wu, D.; Han, C.; et al. Analyzing the Phosphorus Flow Characteristics in the Largest Freshwater Lake (Poyang Lake) Watershed of China from 1950 to 2020 through a Bottom-up Approach of Watershed-Scale Phosphorus Substance Flow Model. *Water Res.* **2023**, *245*, 120546. [CrossRef]
34. Chen, X.; Zheng, L.; Zhu, M.; Jiang, C.; Dong, X.; Chen, Y. Quantitative Identification of Nitrate and Sulfate Sources of a Multiple Land-Use Area Impacted by Mine Drainage. *J. Environ. Manag.* **2023**, *325*, 116551. [CrossRef]
35. Ministry of Ecology and Environment. Implementation Plan for the Special Investigation and Remedial Action on the "Three Phosphorus" of the Yangtze River. EB/OL. Available online: https://www.gov.cn/xinwen/2019-05/02/content_5388260.htm (accessed on 2 May 2019).
36. Honglu, Q.; Jinxin, L.; Yunping, Y.; Liu, Y.; Chai, Y. Quantitative Study of Climatic and Anthropogenic Contributions to Streamflow and Sediment Load in the Yangtze River, China. *Water* **2022**, *14*, 3104. [CrossRef]
37. *HJ/T 103-2003*; Total Phosphorus Water Quality Automatic Analyzer Technical Requirements. China National Institute of Standardization: Beijing, China, 2003.
38. *HJ/T 96-2003*; pH Water Quality Automatic Analyzer Technical Requirements. China National Institute of Standardization: Beijing, China, 2003.
39. *HJ/T 98-2003*; Turbidity Water Quality Automatic Analyzer Technical Requirements. China National Institute of Standardization: Beijing, China, 2003.
40. *HJ/T 99-2003*; Dissolved Oxygen (DO) Water Quality Automatic Analyzer Technical Requirements. China National Institute of Standardization: Beijing, China, 2003.
41. *HJ/T 97-2003*; Conductivity Water Quality Automatic Analyzer Technical Requirements. China National Institute of Standardization: Beijing, China, 2003.
42. *GB/T 13195-1991*; Water Quality Determination of Water Temperature Thermometer or Inverted Thermometer Method. China National Institute of Standardization: Beijing, China, 1991.
43. Zhuo, T.; He, L.; Chai, B.; Zhou, S.; Wan, Q.; Lei, X.; Zhou, Z.; Chen, B. Micro-Pressure Promotes Endogenous Phosphorus Release in a Deep Reservoir by Favouring Microbial Phosphate Mineralisation and Solubilisation Coupled with Sulphate Reduction. *Water Res.* **2023**, *245*, 120647. [CrossRef]
44. Liu, S.; He, G.; Fang, H.; Xu, S.; Bai, S. Effects of Dissolved Oxygen on the Decomposers and Decomposition of Plant Litter in Lake Ecosystem. *J. Clean. Prod.* **2022**, *372*, 133837. [CrossRef]

45. Ahmad, N.; Youjin, L.; Hdia, M. The Role of Innovation and Tourism in Sustainability: Why Is Environment-Friendly Tourism Necessary for Entrepreneurship? *J. Clean. Prod.* **2022**, *379*, 134799. [CrossRef]
46. Zhao, J.; Li, G.; Zhu, Z.; Hao, Y.; Hao, H.; Yao, J.; Bao, T.; Liu, Q.; Yeh, T.-C.J. Analysis of the Spatiotemporal Variation of Groundwater Storage in Ordos Basin Based on GRACE Gravity Satellite Data. *J. Hydrol.* **2024**, *632*, 130931. [CrossRef]
47. Li, Z.; Rao, Z.; Pan, L.; Xu, Z. MTS-Mixers: Multivariate Time Series Forecasting via Factorized Temporal and Channel Mixing. *arXiv* **2023**, arXiv:2302.04501v1.
48. Wang, Y.; Zhang, N.; Wang, D.; Wu, J. Impacts of Cascade Reservoirs on Yangtze River Water Temperature: Assessment and Ecological Implications. *J. Hydrol.* **2020**, *590*, 125240. [CrossRef]
49. Zheng, N.; Li, Z.; Xia, X.; Gu, S.; Li, X.; Jiang, S. Estimating Line Contaminant Sources in Non-Gaussian Groundwater Conductivity Fields Using Deep Learning-Based Framework. *J. Hydrol.* **2024**, *630*, 130727. [CrossRef]
50. Kong, Z.; Song, Y.; Xu, M.; Yang, Y.; Wang, X.; Ma, H.; Zhi, Y.; Shao, Z.; Chen, L.; Yuan, Y.; et al. Multi-Media Interaction Improves the Efficiency and Stability of the Bioretention System for Stormwater Runoff Treatment. *Water Res.* **2024**, *250*, 121017. [CrossRef] [PubMed]
51. Shi, Z.; Du, Y.; Liu, H.; Deng, Y.; Gan, Y.; Xie, X. Molecular Characteristics of Dissolved Organic Phosphorus in Watershed Runoff: Coupled Influences of Land Use and Precipitation. *J. Environ. Sci.* **2025**, *148*, 387–398. [CrossRef]
52. Waller, D.M.; Meyer, A.G.; Raff, Z.; Apfelbaum, S.I. Shifts in Precipitation and Agricultural Intensity Increase Phosphorus Concentrations and Loads in an Agricultural Watershed. *J. Environ. Manag.* **2021**, *284*, 112019. [CrossRef]
53. Lian, M.; Wang, J.; Wang, B.; Xin, M.; Lin, C.; Gu, X.; He, M.; Liu, X.; Ouyang, W. Spatiotemporal Variations and the Ecological Risks of Organophosphate Esters in Laizhou Bay Waters between 2019 and 2021: Implying the Impacts of the COVID-19 Pandemic. *Water Res.* **2023**, *233*, 119783. [CrossRef]
54. Li, Y.; Huang, S.; Fang, P.; Liang, Y.; Wang, J.; Xiong, N. Vegetation Net Primary Productivity in Urban Areas of China Responded Positively to the COVID-19 Lockdown in Spring 2020. *Sci. Total Environ.* **2024**, *916*, 169998. [CrossRef]
55. Ali Shah, S.A.; Longsheng, C.; Solangi, Y.A.; Ahmad, M.; Ali, S. Energy Trilemma Based Prioritization of Waste-to-Energy Technologies: Implications for Post-COVID-19 Green Economic Recovery in Pakistan. *J. Clean. Prod.* **2021**, *284*, 124729. [CrossRef]
56. Wang, Z.; Qu, C.; Zhang, J.; Zhi, L.; Tang, T.; Yao, H.; Li, W.; Shi, C.; Qi, S. Constructing Model-Averaging Species Sensitivity Distributions of Phenanthrene Based on Reproductive Fitness: Implications for Assessing Ecological Risk in Urban Watershed. *J. Hazard. Mater.* **2023**, *443*, 130296. [CrossRef]
57. Wu, W.; Wang, J.; Wang, H.; Liu, J.; Yao, Q.; Yu, Z.; Ran, X. Trends in Nutrients in the Changjiang River. *Sci. Total Environ.* **2023**, *872*, 162268. [CrossRef]
58. Liu, X.; Tao, K.; Sun, J.; He, C.; Cui, J.; Chen, X. The Introduction of Woody Plants for Freshwater Wetland Restoration Alters the Archaeal Community Structure in Soil. *Land Degrad. Dev.* **2017**, *28*, 1933–1942. [CrossRef]
59. Li, J.; Wang, X.; Wu, L. Research on Sediment Deposition Characteristics and the Vegetation Restoration of Ecological Riverbanks in the Deep Waterway Regulation Scheme of Yangtze River. *Water* **2024**, *16*, 2350. [CrossRef]
60. Yan, Z.; Kamanmalek, S.; Alamdari, N. Predicting Coastal Harmful Algal Blooms Using Integrated Data-Driven Analysis of Environmental Factors. *Sci. Total Environ.* **2024**, *912*, 169253. [CrossRef] [PubMed]
61. Reeve, D.; Li, Y.; Lark, M.; Simmonds, D. An Investigation of the Multi-Scale Temporal Variability of Beach Profiles at Duck Using Wavelet Packet Transforms. *Coast. Eng.* **2007**, *54*, 401–415. [CrossRef]
62. Chen, Y.; Huang, L.; Xie, X.; Liu, Z.; Hu, J. Improved Prediction of Hourly PM2.5 Concentrations with a Long Short-Term Memory and Spatio-Temporal Causal Convolutional Network Deep Learning Model. *Sci. Total Environ.* **2024**, *912*, 168672. [CrossRef]
63. Yao, J.; Chen, S.; Ruan, X. Interpretable CEEMDAN-FE-LSTM-Transformer Hybrid Model for Predicting Total Phosphorus Concentrations in Surface Water. *J. Hydrol.* **2024**, *629*, 130609. [CrossRef]
64. Payne, M.R.; Danabasoglu, G.; Keenlyside, N.; Matei, D.; Miesner, A.K.; Yang, S.; Yeager, S.G. Skilful Decadal-Scale Prediction of Fish Habitat and Distribution Shifts. *Nat. Commun.* **2022**, *13*, 2660. [CrossRef]
65. Han, L.; Ye, H.-J.; Zhan, D.-C. The Capacity and Robustness Trade-off: Revisiting the Channel Independent Strategy for Multivariate Time Series Forecasting. *arXiv* **2023**, arXiv:2304.05206v1. [CrossRef]
66. Xu, C.; Chen, X.; Zhang, L. Predicting River Dissolved Oxygen Time Series Based on Stand-Alone Models and Hybrid Wavelet-Based Models. *J. Environ. Manag.* **2021**, *295*, 113085. [CrossRef]
67. Kasiviswanathan, K.S.; He, J.; Sudheer, K.P.; Tay, J.-H. Potential Application of Wavelet Neural Network Ensemble to Forecast Streamflow for Flood Management. *J. Hydrol.* **2016**, *536*, 161–173. [CrossRef]
68. Zhang, H.; Zhou, X.; Lv, X.; Xu, X.; Weng, Q.; Lei, K. Exploration of the Factors That Influence Total Phosphorus in Surface Water and an Evaluation of Surface Water Vulnerability Based on an Advanced Algorithm and Traditional Index Method. *J. Environ. Manag.* **2023**, *342*, 118155. [CrossRef] [PubMed]
69. Zhang, X.; Liang, F.; Srinivasan, R.; Van Liew, M. Estimating Uncertainty of Streamflow Simulation Using Bayesian Neural Networks. *Water Resour. Res.* **2009**, *45*, 2008WR007030. [CrossRef]

70. Xu, J.; Xu, M.; Zhao, Y.; Wang, S.; Tao, M.; Wang, Y. Spatial-Temporal Distribution and Evolutionary Characteristics of Water Environment Sudden Pollution Incidents in China from 2006 to 2018. *Sci. Total Environ.* **2021**, *801*, 149677. [CrossRef]
71. Zeng, A.; Chen, M.; Zhang, L.; Xu, Q. Are Transformers Effective for Time Series Forecasting? *arXiv* **2022**, arXiv:2205.13504. [CrossRef]
72. Liu, M.; Zeng, A.; Chen, M.; Xu, Z.; Lai, Q.; Ma, L.; Xu, Q. SCINet: Time Series Modeling and Forecasting with Sample Convolution and Interaction. *arXiv* **2022**, arXiv:2106.09305.
73. Lee-Thorp, J.; Ainslie, J.; Eckstein, I.; Ontanon, S. FNet: Mixing Tokens with Fourier Transforms. *arXiv* **2022**, arXiv:2105.03824.